# Dynamic Analysis of a 13-Story Steel Frame Building Instrumented and Damaged in the 1994 Northridge Earthquake

**Chia-Ming Uang [1], Qi-song Yu[1], Ali Sadre [2], David Bonowitz[3], and Nabih Youssef [3]**

## ABSTRACT

This case study is for an instumented thirteen-story steel moment frame (SMF) building located near the epicenter, which sustained damage to its welded connections during the 1994 Northridge earthquake. The building, which was instrumented on three floors, had been surveyed and data was collected on the fractured joints. One objective of this study was to verify the accuracy of present analytical tools in predicting the extent and severity of connection failures. Elastic time-history analysis showed good correlation with the measured response in E-W direction. In the other direction with strong ground shaking, panel zones had to be modeled in the inelastic time-history analysis in order to achieve good correlation. The inelastic analysis indicated that panel zones must have been a major source of energy dissipation during the Northridge earthquake. From this study, it appears that current analytical tools for both elastic and inelastic analyses can be instrumental in predicting the intensity and pattern of the expected damage during severe seismic events.

## INTRODUCTION

The 1994 Northridge event has afforded an opportunity to investigate issues like: near-field effects and cumulative damage; impact from the vertical component of the ground motion; significance of the higher modes and building irregularities; importance of redundancy, overstrength and its relation to rotation ductility demands; influence of slabs and panel zone flexibility; adequacy of available analytical or modeling tools and related design assumptions to accurately predict the extent and location of the observed damage in buildings. The main objective of this paper is to establish the adequacy of current modeling techniques to predict the pattern and the extent of the connection damage observed after the Northridge Earthquake.

## BUILDING DESCRIPTION AND AVAILABLE DATA

**Building Location and Sturctural System:** The case study is for a thirteen-story SMF office building in the San Fernando Valley, built under the 1973 UBC. Lateral stiffness and resistance are provided by SMFs on the perimeter. Figure 1 shows the elevation indicating typical frame member sizes and the story heights. The building is square shaped in plan and box columns are used at the corners. The typical floor and roof system is composite slab. A uniformly distributed dead load of 72.5 psf with 20 psf curtain wall weight was used for reactive mass calculations.

[1] University of California, San Diego
[2] Esgil Corporation, San Diego
[3] Nabih Youssef & Associates, Los Angeles

**Observed Damage:** Damage pattern to the west side frame of the building is summarized in Figure 1. Joint fractures on this side were more prevalent than the other three sides (Uang et al. 1995). Definition of various damage patterns is depicted in Figure 2. Figure 1 illustrates that the damaged connections were essentially classified as types $C_5$, $G_3$, $W_1$, and $W_4$. A controversial type of damage, $W_1$ signifies a crack at the root of the weld, detectable by ultrasonic testing (UT). It is considered a rejectable planar discontinuity of class B or C, per American Welding Society Standards D1.1 (AWS 1994). This type of crack is ordinarily visible once the backing bar is removed. Some speculate that $W_1$ cracks may easily be misread or could have existed before the earthquake.

**Strong Motion Records:** Strong motion recording instruments are located on the basement level, the sixth floor, and the twelfth floor. See Figure 3 for recorded accelerations provided by CDMG (Darragh et al. 1994). The peak horizontal accelerations at the basement were 0.41g and 0.32g in the N-S and E-W directions, respectively.

## ELASTIC ANALYSES

**Objectives:** The main objectives of conducting elastic time-history analyses were (1) to correlate the structure's predicted and recorded responses, (2) to compute demand/capacity ratios (DCRs) of beams and columns and correlate with observed damage, and (3) to compute response envelopes for lateral displacements and maximum story drift ratios.

**Modeling Assumptions:** The following assumptions were made based on the SAC benchmark guidelines: bare steel frame with centerline dimensions and no accidental torsion; use expected yield stress ($F_y$= 47 ksi) to compute member strength; use LRFD (1994) with $\phi$ = 1 for calculating DCRs; use 1.0D + 0.5L + 1.0E load case; consider orthogonal effects per 1991 UBC; and consider P-$\Delta$ effects.

**Input Ground Motions:** The basement record, i.e., the Oxnard record, was used as the input motion for both elastic and inelastic time-history correlations. Furthermore, the Sylmar (i.e., Olive View Hospital) record with a peak ground acceleration of 0.84g was also used to predict deformation demand of the structure.

**Elastic Time-History Correlation:** Translational natural periods were computed from a 3-D model, by SAP90 (Wilson and Habibullah 1992), to be 2.9, 1.0, and 0.6 seconds in the first three modes. Figure 4 indicates that elastic analysis correlates well with the measured response in the E-W direction, but not so well in the N-S direction due to more severe shaking in this direction. The DCRs were also computed. Figure 5 shows the maximum DCR in the N-S frame beams as 1.24, double that in the E-W direction. Beams with higher DCRs are located between levels 2 and 6, correlating reasonably well with the observed damage on the west side frame in Figure 1.

**Interpretation of Damage Data Based on DCRs:** Some standardizations are made to establish statictical correlations with other buildings with similar plots (Youssef et al. 1995). The elastic beam DCRs are normalized by the maximum building DCR and labeled as NRDCR (see Figure 6). Observe that the maximum beam DCR is 1.24, the mean DCR is 0.64 with a standard

deviation of 0.32, and the normalized average of 0.64/1.24=0.52. The connections are generally categorized for the bottom girder-flange damage (BG). Thus "BGC" damage indicates fracture in BG, or in adjacent column flange (BC). Similarly, "BGCW" connections have BGC damage, or bottom weld fracture (BW). Finally, "$BGCWW_1$" damage includes the above and root cracks at the bottom weld.

*Damage Distribution and DCRs:* Out of 551 total inspected connections, 22 were found to have BGC damage, 12 had BW damage (thus, BGCW=34), and 20 had $BW_1$ cracks, which results in $BGCWW_1$=54 (see Figure 6a). Clearly, most of the serious BGC damage is in connections with high DCRs. While this does not necessarily mean that high stresses caused fracture, i.e., fractures not simulated by the elastic model may have occurred at low stresses, it does suggest a useful relationship between the analytical demand and the observed damage.

*Cummulative Damage by DCRs:* Cumulative distribution of damage subsets by NRDCR are depicted in terms of fractions in Figure 6b. Here 1.00 represents 551 total connections, 22 BGC, 34 BGCW, or 54 $BGCWW_1$ in respective categories. If damage was not related to DCR, one would expect the curve for any reasonably sized subset of connections to follow the curve of "All" connections. The steep slope of the BGC curve, at the right end, strongly suggests that this critical damage is closely tied to DCR. Further, when BW and $BW_1$ damage are added, the subset curves approach the "All" curve, suggesting that root cracks are less related to DCR.

*Damage Distribution Ratios:* The ratio of damaged connections to total connections for each group are shown in Figure 6c with DCR larger than those plotted on the abscissa. For example, the BGC ratio at DCR=0.7 is about 0.1, i.e., 10% of all connections with DCR $\geq$ 0.7 have BGC damage. While the $BGCWW_1$ ratio doubles as DCR increases from zero to 1.0, the BGC ratio increases from 4% to 20%. If $BW_1$ and BGCW fractures were not related, one would find at least some root cracks in each DCR group. However, no $BW_1$ damage is found among the 108 connections with DCR $\geq$ 0.9. This suggests that original defects in connections became fractures during the earthquake. Also the overall $BW_1$ ratio is only about 4%, much lower than 20% BGCW for high DCRs, suggesting that poor initial quality alone is not sufficient to cause damage even under high stresses. The patterns of damage seem to be both *quality-based* and *demand-based;* the question is how are the two linked.

**Response Envelopes:** Time-history analyses were conducted to obtain the envelopes of both story drift ratios and lateral displacements. In the N-S direction, the Oxnard record produces a roof drift ratio of 1.1% with a story drift ratio as high as 1.7%. The Sylmar record produces a roof drift ratio of 2.0% and a story drift ratio of 2.7% (see Figure 7).

**Observations:** For the N-S component of the Oxnard record, floor levels 2 through 7 with story drift ratios larger than 1.3% correspond to DCRs $\geq$ 1.0 and correlate reasonably well with the observed damage in the N-S frame. Thus, it appears that both story drfit ratios and DCRs are reliable indicators of the damage pattern.

## INELASTIC ANALYSES

**Objectives:** The main objectives of conducting inelastic time-history analyses were to (1) correlate the recorded and predicted responses, (2) to predict stroy drifts, plastic rotation demands in beams, columns, and panel zones, and (3) to correlate predicted response with observed damage.

**Modeling Assumptions:** The DRAIN-2DX (Prakash et al. 1993) computer program was used. Beams and columns with rigid offsets were modeled by Element 2, while semi-rigid Element 4 was used to model panel zones (Krawinkler 1978). Rayleigh damping with a 5% damping factor was assigned to the first and third modes and a 2% strain hardening ratio was assumed for beams.

**Inelastic Time-History Correlation:** With the basement record of the building as the input motion, the predicted lateral displacements are compared with the recorded displacements (see Figure 8).

In the E-W direction, a comparison of Figures 8a and 4a (elastic analysis) indicates a slight improvement in the correlation. In the N-S direction — a direction of strong shaking and significant damage — a comparison of Figures 8b and 4b shows a very dramatic improvement in the correlation with a much closer matching in amplitude and phase. The plastic rotation demand for the N-S component of the Oxnard record is depicted in Figure 9a; note that most of the yielding is concentrated in the panel zones. The maximum plastic rotations in the panel zones and beams are 0.013 and 0.006 radians, respectively.

It appears from this dynamic analysis that panel zones must have played a very important role in dissipating energy during the 1994 Northridge earthquake, although shear yielding with the magnitue of plastic rotation demand shown in Figure 9a is difficult to detect visually in the field. To test this hypothesis, a separate inelastic time-history analysis was conducted without modeling the panel zones, which worsened the correlation between the predicted and recorded response (see Figure 10).

**Story Drift Ratios and Plastic Rotation Demand:** Figure 11 shows the envelopes of lateral displacements and story drift ratios for both the Oxnard and Sylmar records. The maximum story drift ratios produced by the Oxnard and Sylmar records were about 1.6% and 2% while the roof drift ratios were around 0.75% and 1.1%, respectively. The maximum panel zone plastic rotation is 0.013 radians for the Oxnard record (see Figure 9a) and is 0.015 radians for the Sylmar record (see Figure 12a).

## CONCLUSIONS

Based on the results of time-history analyses, recorded building response, and observed joint damage, the following conclusions can be drawn.

**Elastic Analyses:** The SAP90 elastic analyses, which considered the center-line dimension bare steel frames in the perimeter of the building, resulted in the following conclusions.

(1) The elastic response correlated very well with the measured building response in the E-W direction. The intensity of the basement motion in the N-S direction was about 50% higher

than that in the E-W direction. Since the elastic model could not simulate the yielding and damage of moment connections, the elastic time-history correlation was poor in the N-S direction.

(2) Demand/capacity ratios (DCRs) computed from the elastic model provided a reasonable correlation to the observed damage. Field inspections and survey data indicated generally a higher incidence of welded connection failure in the N-S direction as oppose to the E-W direction. The maximum DCRs were 1.24 and 0.63 in the N-S and E-W directions, respectively.

(3) Frame members with higher DCRs were concentrated between floor levels 2 and 6, which correlated reasonably well with the observed damage to the west side frame in the N-S direction.

(4) The Sylmar record has much higher damage potential to the building frame. The maximum DCR was about 2, the maximum roof drift ratio was nearly 2.0%, and the maximum story drift ratio was around 2.7%.

**Inelastic Analyses:** The mathematical model for the DRAIN-2DX inelastic analyses incorporated panel zone elements. The following conclusions can be made.

(1) The DRAIN-2DX time-history analysis drastically improved the correlation in the N-S direction. For the type of regular building investigated in this study, DRAIN-2DX or similar computer programs is a very useful tool to predict the seismic damage and deformation demand of steel moment frames.

(2) The time-history correlation study indicated that most of the inelastic actions were concentrated in the panel zones, not beams. It implies that panel zones must have played an important role to dissipate earthquake input energy during the Northridge earthquake.

(3) The maximum story drift ratio and plastic rotation that developed during the Northridge earthquake were estimated to be 1.6% and 0.013 radians, respectively. The sylmar record would produce a stroy drift ratio of 2% and a plasitc rotation of 0.015 radians.

## ACKNOWLEDGEMENTS

This report was made possible by a grant through the SAC Joint Venture, which is a cooperative effort between the Structural Engineers Association of California (SEAOC), Applied Technology Council (ATC) and California State Universities for Research in Earthquake Engineering (CUREe). Also thanks to Dr. Huang with the Office of Strong Motion Studies, Division of Mines and Geology, Department of Conservation for providing the processed records.

## REFERENCES


1. AISC, *Load and resistance factor design (LRFD)*, Amer. Inst. of Steel Constr., Chicago, Ill., 1994.
2. AWS, "Structural welding code - steel," *ANSI/AWS D1.1 - 94*, AWS, Miami,FL., 1994.
3. Krawinkler, H., "Shear in beam-column joints in seismic design of steel frames," *Engrg.J.* vol. 15, no. 3, 1978.
4. Prakash, V., Powell, G.H., and Filippou, F.C., "DRAIN-2DX," *User Guide*, U. C. Berkeley, Ca., 1993.
5. Uang, C.-M., Yu, Q.-S., Sadre, A., Bonowitz, D., and N. Youssef, "Performance of a 13-story steel moment-resisting frame damaged in the 1994 Northridge earthquake," Report No. SSRP-95/04, Univ. Of Calif., San Diego, La Jolla, CA, 1994.
6. *Uniform Building Code (UBC)*, Int. Conf. of Bldg. Officials, Whittier, Calif., 1991.
7. Wilson, E. L. and Habibullah, A., *SAP90 - Structural analysis users manual*, CSI, Berkeley, CA, 1992
8. Youssef, N. F. G., Bonowitz, D., and Gross, J. L., "A survey of steel moment-resisting frame buildings affected by the 1994 Northridge earthquake," *Report No. NISTIR 5625*, NIST, Gaithersburg, MD, 1995.

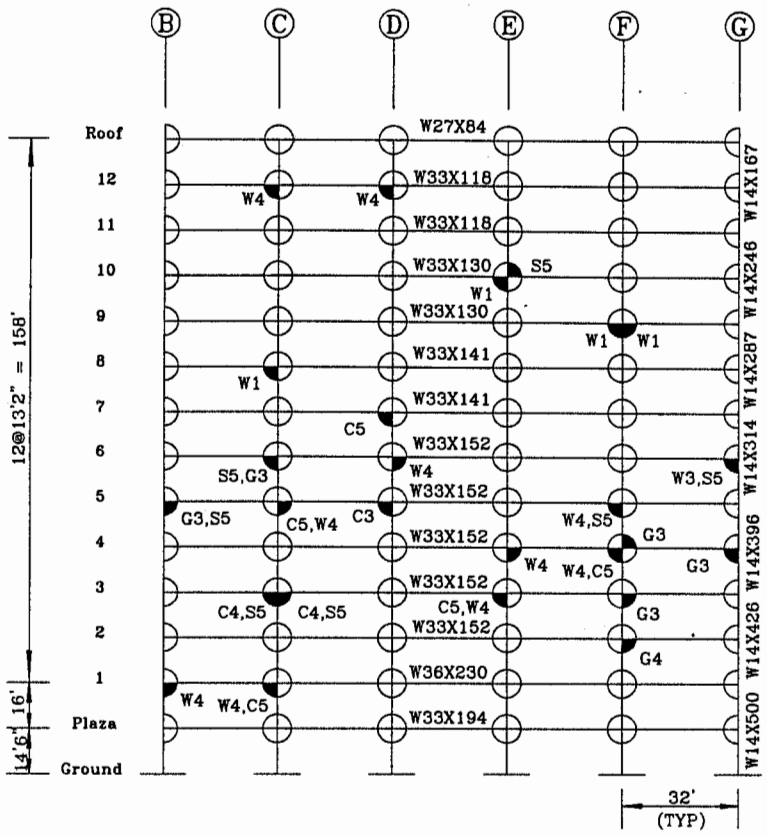


Figure 1 Elevation and Damage Pattern of the Frame (West Side)

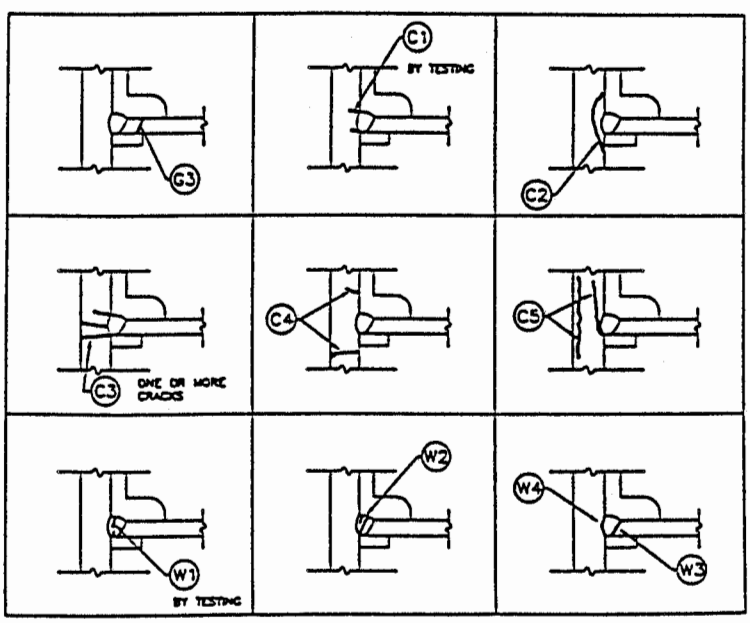


Figure 2 Moment-Resisting Frame Damage Type

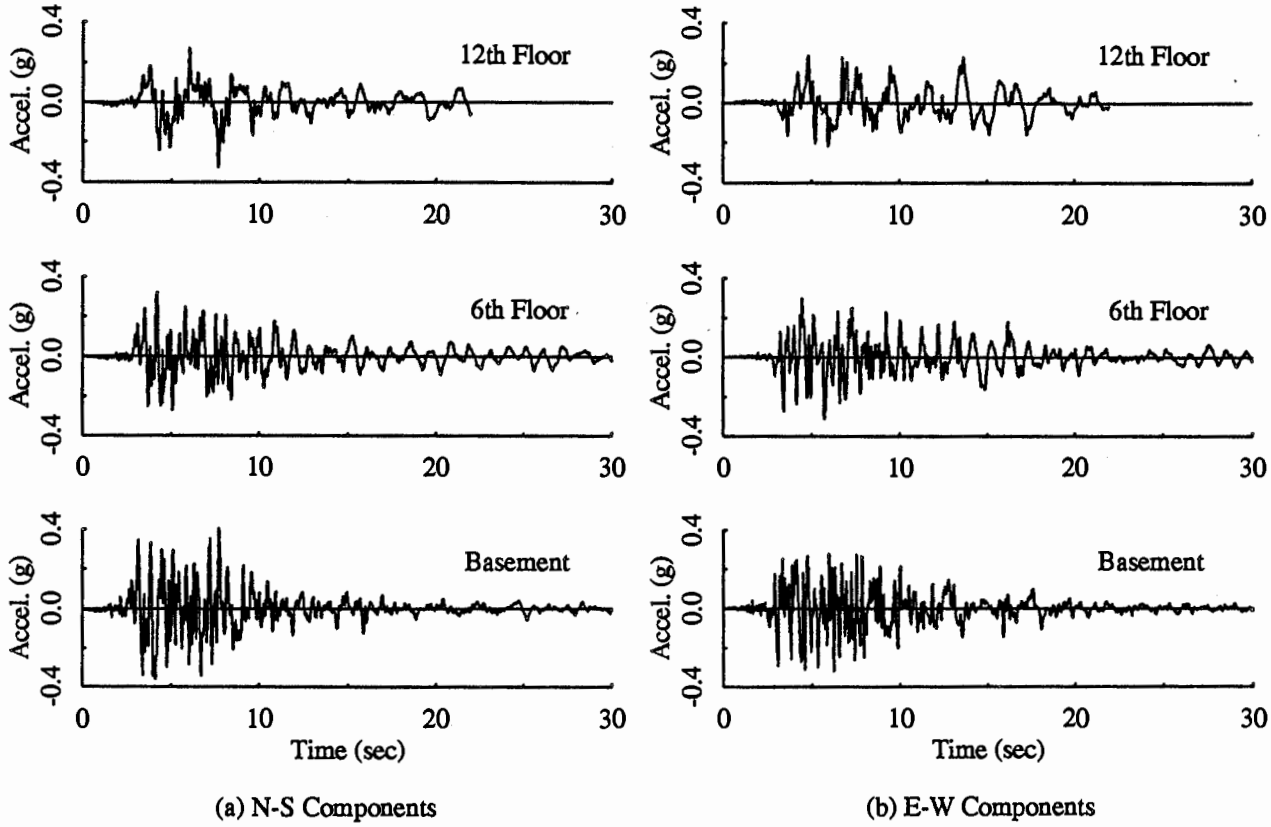


(a) N-S Components (b) E-W Components

Figure 3 Recorded Absolute Accelerations (Oxnard Record, 1994 Northridge)

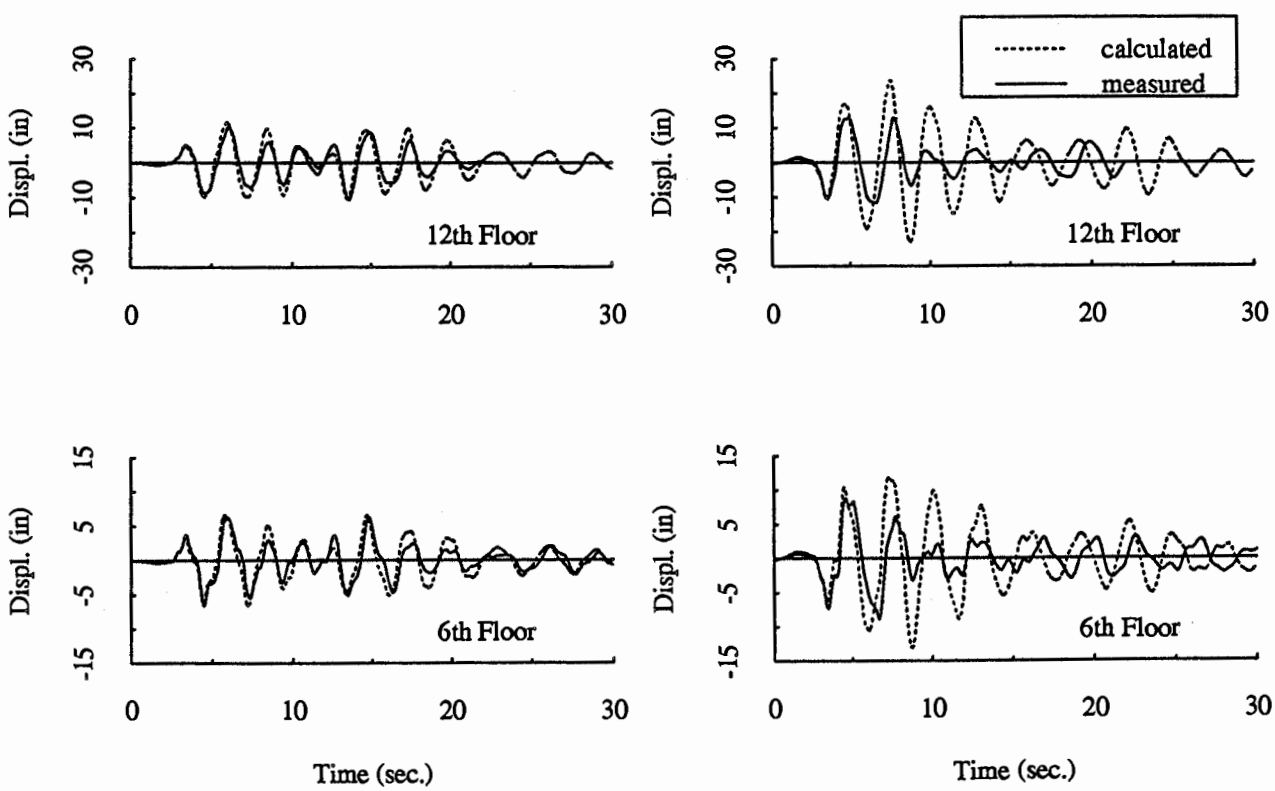


(a) E-W Direction (b) N-S Direction

Figure 4 Elastic Time-History Correlation (Oxnard Record, 1994 Northridge)

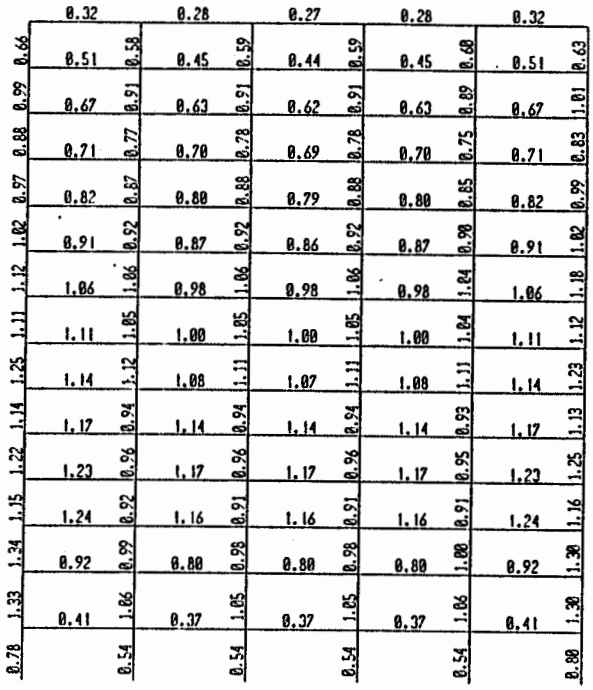


Figure 5 Demand/Capacitiy Ratio (N-S)

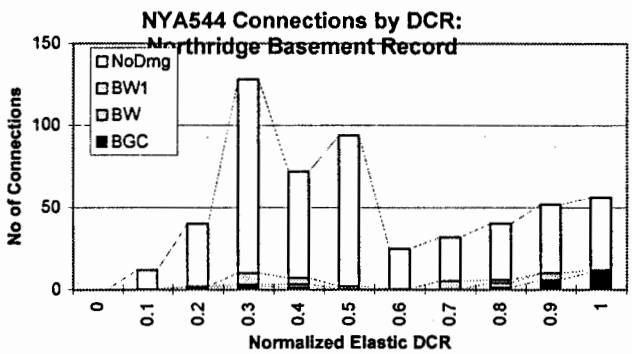


| Distribution of Inspected and Analyzed (Case 6) Connections by Normalized DCR | | | | | | | |
|---|---|---|---|---|---|---|---|
| NRDCR | ALL | BGC | BGCW | BGCWW1 | BW | BW1 | No Dmg |
| 0 | 0 | 0 | 0 | 0 | 0 | 0 | 0 |
| 0.1 | 12 | 0 | 0 | 0 | 0 | 0 | 12 |
| 0.2 | 40 | 1 | 2 | 2 | 1 | 0 | 38 |
| 0.3 | 128 | 2 | 3 | 10 | 1 | 7 | 118 |
| 0.4 | 72 | 1 | 3 | 7 | 2 | 4 | 65 |
| 0.5 | 94 | 0 | 0 | 2 | 0 | 2 | 92 |
| 0.6 | 25 | 0 | 0 | 0 | 0 | 0 | 25 |
| 0.7 | 32 | 0 | 0 | 5 | 0 | 5 | 27 |
| 0.8 | 40 | 1 | 4 | 6 | 3 | 2 | 34 |
| 0.9 | 52 | 6 | 10 | 10 | 4 | 0 | 42 |
| 1 | 56 | 11 | 12 | 12 | 1 | 0 | 44 |
| Total: | 551 | 22 | 34 | 54 | 12 | 20 | 497 |

(a) Distribution of Inspected and Analyzed Connections with DCRs

Figure 6 Distribution of Inspected Connections with Normalized DCRs (continued)

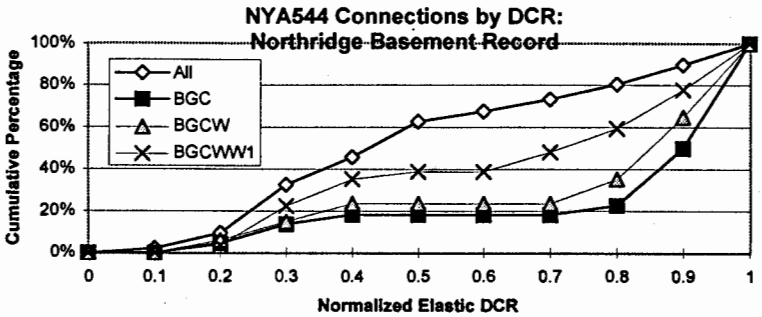


| Cumulative Distribution of Inspected and Analyzed (Case 6) Connections by Normalized DCR | | | | |
|---|---|---|---|---|
| CUMULATIVE VALUES | | | | |
| NRDCR | All | BGC | BGCW | BGCWW1 |
| 0 | 0.00 | 0.00 | 0.00 | 0.00 |
| 0.1 | 0.02 | 0.00 | 0.00 | 0.00 |
| 0.2 | 0.09 | 0.05 | 0.06 | 0.04 |
| 0.3 | 0.33 | 0.14 | 0.15 | 0.22 |
| 0.4 | 0.46 | 0.18 | 0.24 | 0.35 |
| 0.5 | 0.63 | 0.18 | 0.24 | 0.39 |
| 0.6 | 0.67 | 0.18 | 0.24 | 0.39 |
| 0.7 | 0.73 | 0.18 | 0.24 | 0.48 |
| 0.8 | 0.80 | 0.23 | 0.35 | 0.59 |
| 0.9 | 0.90 | 0.50 | 0.65 | 0.78 |
| 1 | 1.00 | 1.00 | 1.00 | 1.00 |

(b) Cumulative Distribution of Inspected Connections with Normalize DCR

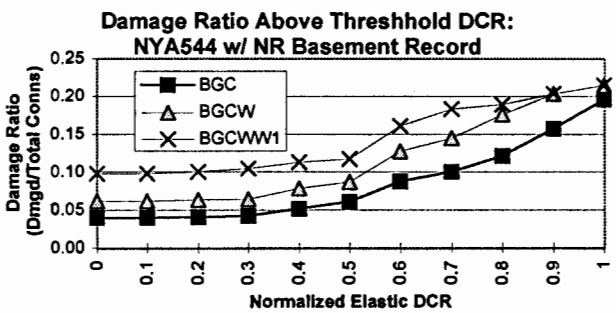


| Damage Ratios of Inspected and Analyzed (Case 6) Connections above Threshold Normalized DCR | | | | | | | |
|---|---|---|---|---|---|---|---|
| NRDCR | All | Cum BGC | Cum BGCW | Cum BGCWW1 | BGC | BGCW | BGCWW1 |
| 0 | 551 | 22 | 34 | 54 | 0.04 | 0.06 | 0.10 |
| 0.1 | 551 | 22 | 34 | 54 | 0.04 | 0.06 | 0.10 |
| 0.2 | 539 | 22 | 34 | 54 | 0.04 | 0.06 | 0.10 |
| 0.3 | 499 | 21 | 32 | 52 | 0.04 | 0.06 | 0.10 |
| 0.4 | 371 | 19 | 29 | 42 | 0.05 | 0.08 | 0.11 |
| 0.5 | 299 | 18 | 26 | 35 | 0.06 | 0.09 | 0.12 |
| 0.6 | 205 | 18 | 26 | 33 | 0.09 | 0.13 | 0.16 |
| 0.7 | 180 | 18 | 26 | 33 | 0.10 | 0.14 | 0.18 |
| 0.8 | 148 | 18 | 26 | 28 | 0.12 | 0.18 | 0.19 |
| 0.9 | 108 | 17 | 22 | 22 | 0.16 | 0.20 | 0.20 |
| 1 | 56 | 11 | 12 | 12 | 0.20 | 0.21 | 0.21 |

(c) Distribution of Damage Ratios

Figure 6 Distribution of Inspected Connections with Normalized DCRs

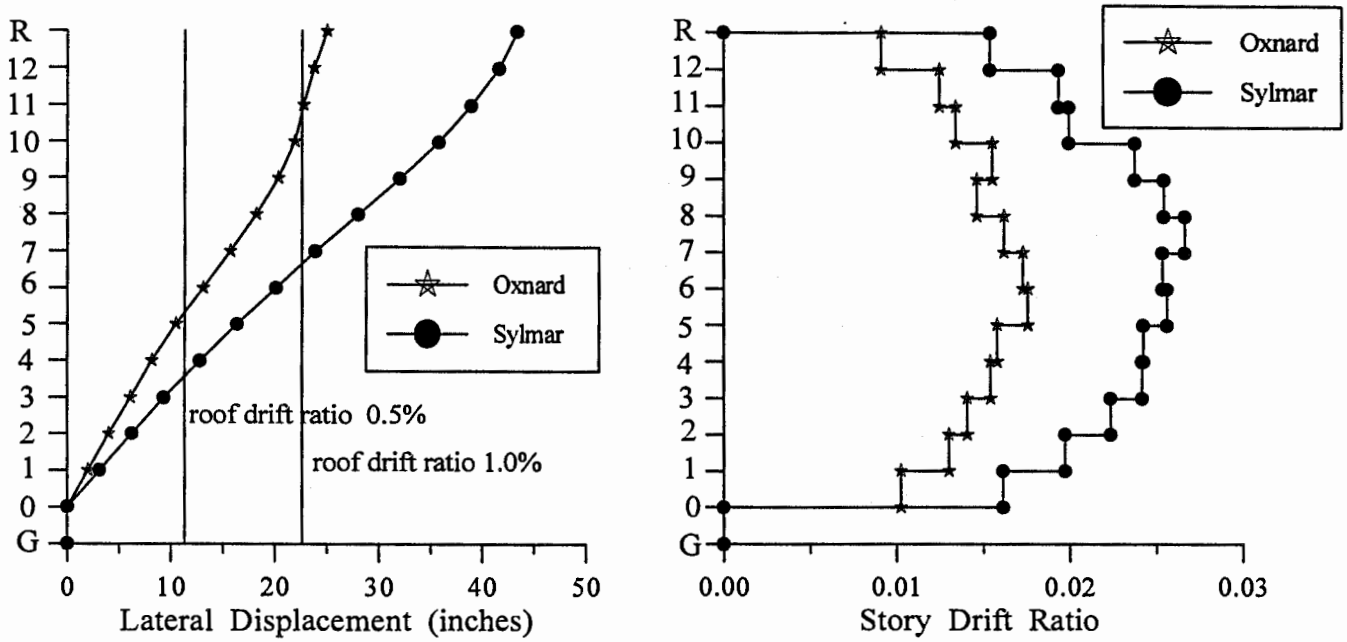


Figure 7 Elastic Response Envelopes (N-S)

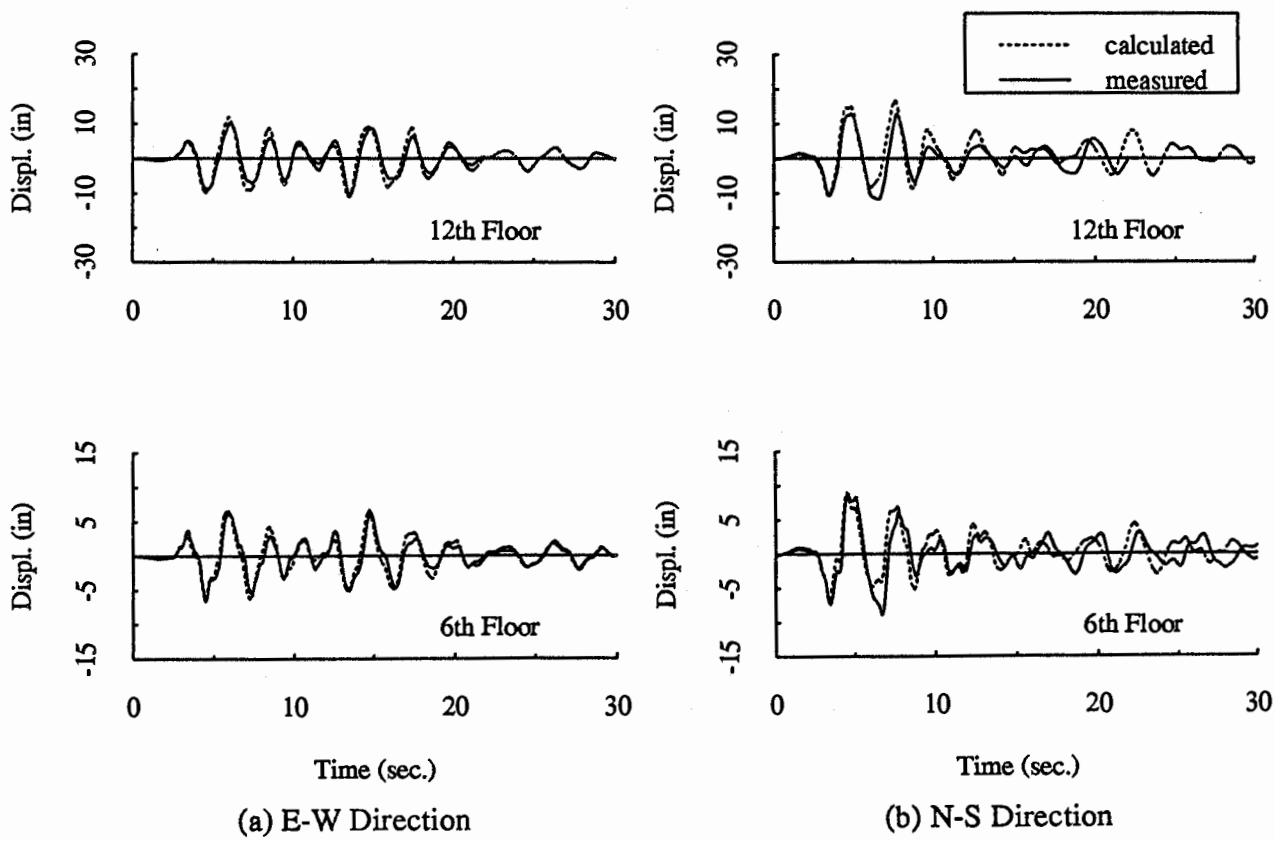


Figure 8 Inelastic Time-History Correlation (Oxnard Record, 1994 Northridge)

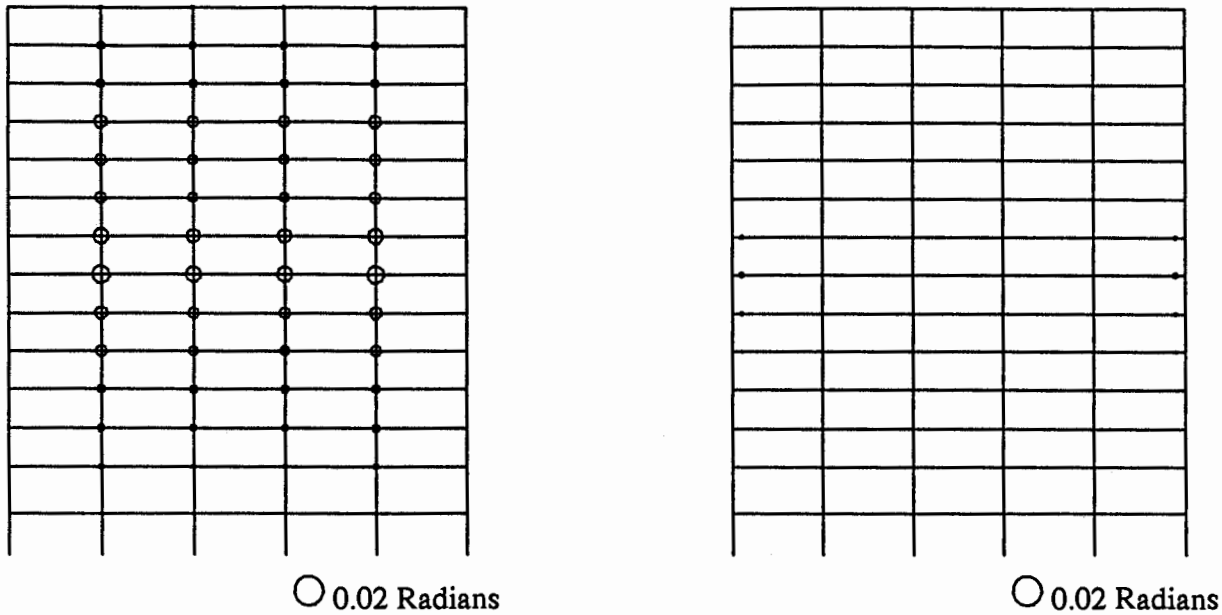


(a) Panel Zones (b) Beams and Columns

Figure 9 Distributions of Maximum Plastic Rotations
(N-S Comp. Of Oxnard Record, 1994 Northridge)

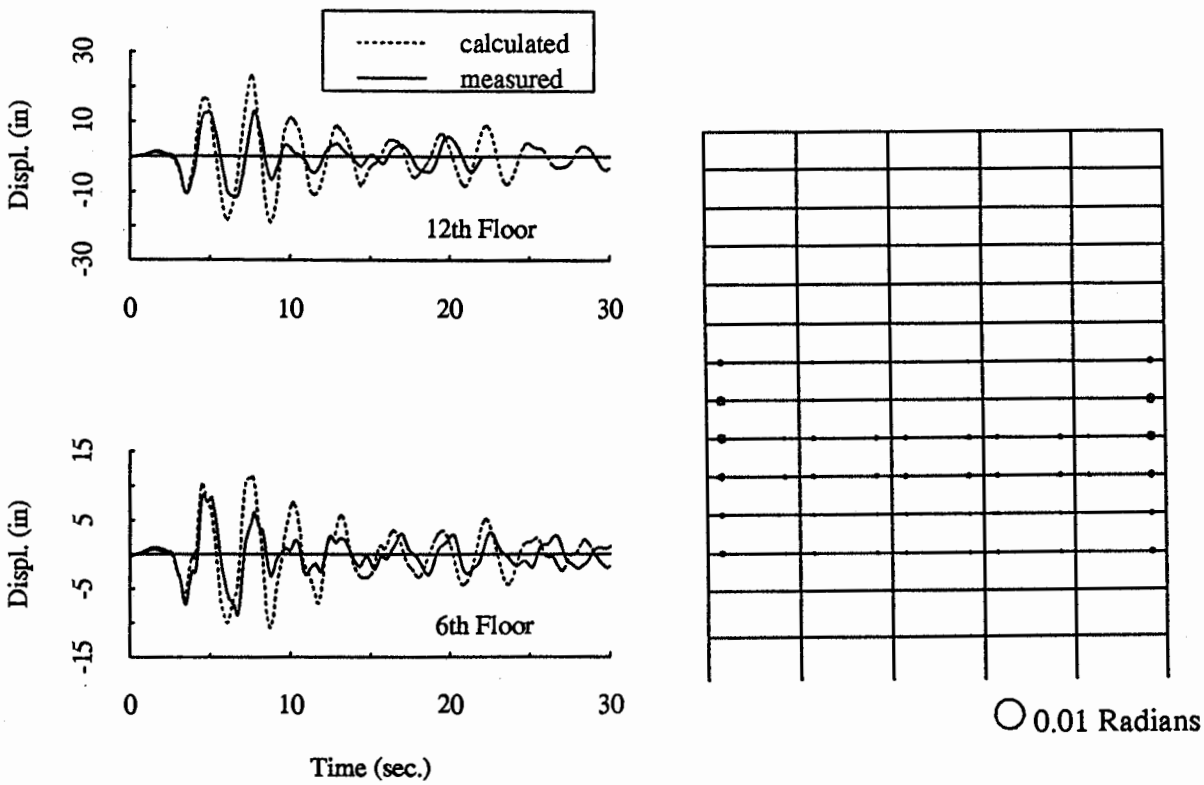


(a) Displacement Time-History Correlation (b) Plastic Rotations

Figure 10 Inelastic Time-History Correlation *without* Modeling Panel Zones

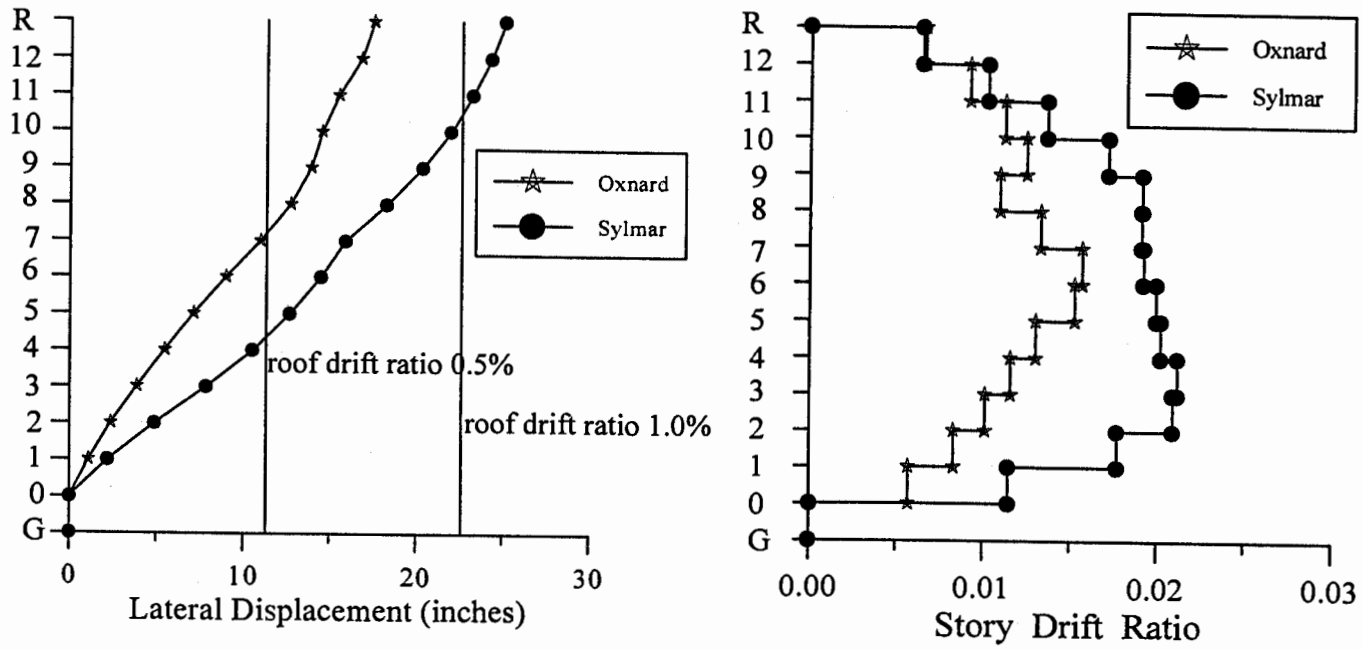


Figure 11 Inelastic Response Envelopes (N-S)

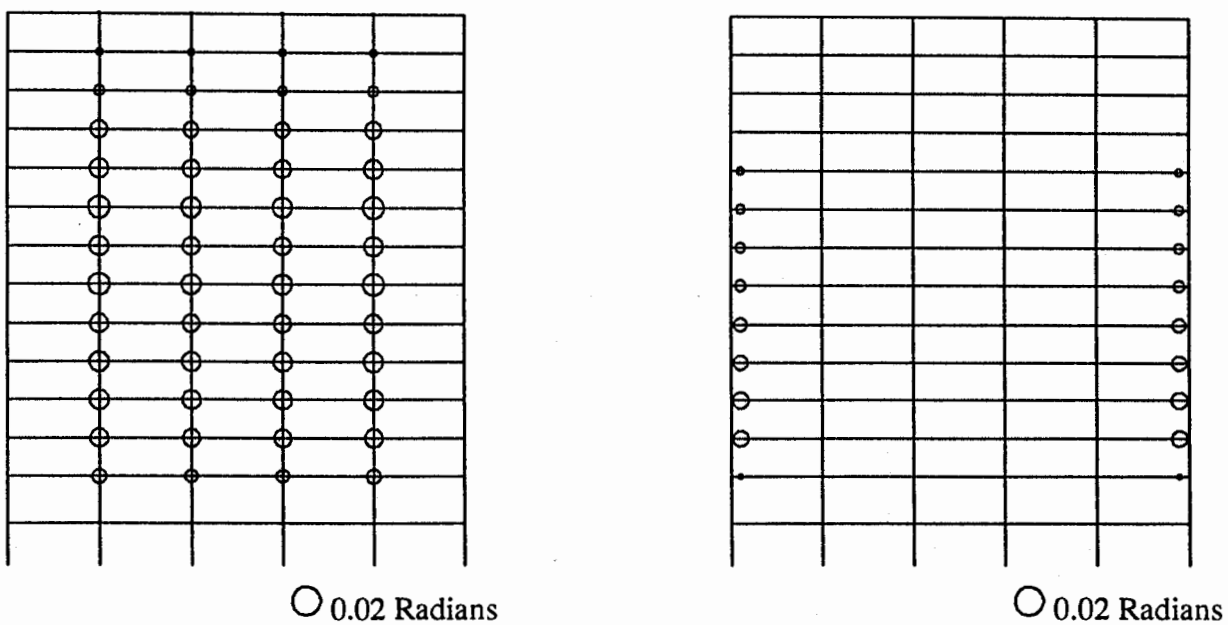


(a) Panel Zones

(b) Beams and Columns

Figure 12 Distributions of Maximum Plastic Rotations
(N-S Comp. Of Sylmar Record, 1994 Northridge)